

**EXPERIMENTAL TOXIC HEPATITIS LEADS TO PROGRESSIVE RETINAL  
NEUROVASCULAR DEGENERATION**

**Gulnoza O. Khidirova**

Associate professor, Department of Anatomy, histology and pathological anatomy,  
Tashkent State medical university, Uzbekistan

**Abboskhon B. Burkhonov**

Department of Anatomy, histology and pathological anatomy,  
Tashkent State medical university, Uzbekistan

**Abstract:** Toxic hepatitis is accompanied by pronounced systemic metabolic disturbances that extend beyond hepatic tissue and involve extrahepatic organs, including the retina. The present study was designed to characterize morphological alterations of the retinal layers in an experimental model of toxic hepatitis and to evaluate the potential protective effects of hepatoprotective therapy. Thirty adult rats were randomly allocated into three groups: intact control, toxic hepatitis, and toxic hepatitis treated with silymarin. Retinal specimens were subjected to histological and histochemical examination using hematoxylin–eosin, periodic acid–Schiff (PAS), Nissl staining, and silver impregnation techniques. Induction of experimental toxic hepatitis led to marked disorganization of retinal laminar architecture, thickening of retinal vascular walls, degeneration of photoreceptor elements, and a significant decrease in ganglion cell density ( $p < 0.05$ ). PAS staining demonstrated enhanced accumulation of glycoprotein components within the walls of retinal microvessels, indicating metabolic and structural vascular impairment. Administration of silymarin resulted in partial attenuation of both vascular and neuronal damage; however, complete restoration of normal retinal morphology was not achieved. Overall, the obtained results indicate that retinal structural alterations mirror systemic toxic injury associated with experimental toxic hepatitis, supporting the retina as a sensitive morphological indicator of extrahepatic manifestations of hepatic pathology.

**Keywords:** Toxic hepatitis; Retina; Retinal morphology; Experimental rats; Silymarin

**Introduction.** Toxic hepatitis is characterized by impaired hepatic detoxification and profound metabolic imbalance, leading to systemic hypoxia, oxidative stress, and vascular dysregulation. These disturbances extend beyond the liver and may affect organs with high metabolic demands. The retina is a highly specialized neurovascular tissue that is particularly sensitive to systemic metabolic and circulatory disturbances. Alterations in retinal microvasculature and neuronal layers have been reported in various systemic pathological conditions, suggesting that retinal morphology may reflect generalized toxic injury. Despite extensive investigation of hepatic pathology in toxic hepatitis, structural changes in the retina remain insufficiently characterized. The present study aimed to evaluate retinal morphostructural alterations in an experimental model of toxic hepatitis and to assess the potential protective effects of hepatoprotective therapy.

**Materials and Methods.** Animals and experimental design. Thirty adult white rats (180–220 g) were used in this study. Animals were housed under standard laboratory conditions with free access to food and water and maintained on a 12-hour light/dark cycle. Rats were randomly divided into three groups ( $n = 10$  per group): Control group, toxic hepatitis group, toxic hepatitis silymarin treatment group. All experimental procedures were conducted in accordance with institutional guidelines for animal care and were approved by the local ethics committee. Experimental toxic hepatitis was induced by intraperitoneal administration of carbon tetrachloride ( $\text{CCl}_4$ ) at a dose of 0.5 ml/100 g body weight, diluted 1:1 with sunflower oil. Injections were administered every other day for 7 days. Control animals received equivalent volumes of sunflower oil. Animals in the treatment group received silymarin orally at a dose of 100 mg/kg/day for 21 consecutive days following induction of toxic hepatitis.

At the end of the experiment, animals were euthanized, and eyeballs were enucleated and fixed in 10% neutral buffered formalin. Tissue samples were processed routinely, embedded in paraffin, and sectioned at 4–5 μm thickness.

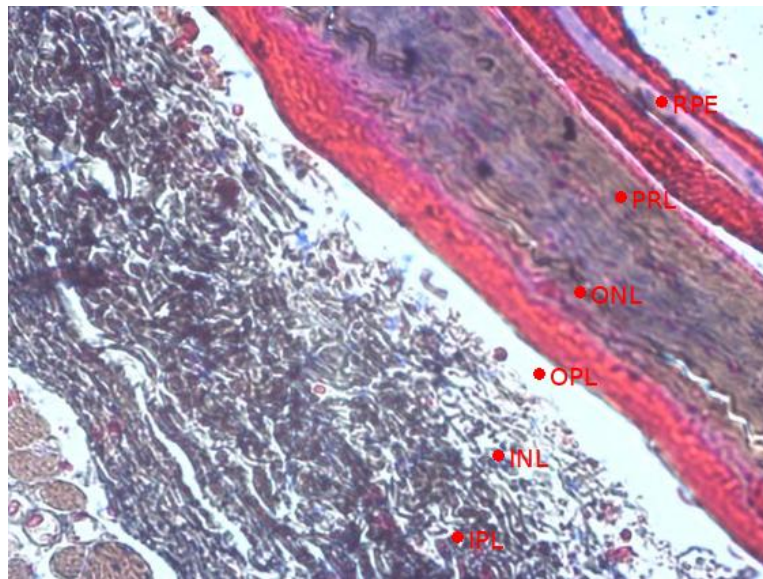


**Fig.1 Azan-stained retinal preparation**

1. Sclera (collagen-rich, blue) 2. Choroid (vascular layer) 3. Retinal pigment epithelium (RPE)
4. Photoreceptor layer 5. Outer nuclear layer 6. Inner nuclear layer

The outer nuclear layer (ONL) contains densely packed nuclei of photoreceptor cells, arranged in regular rows. The outer plexiform layer (OPL) appears as a lightly stained zone with synaptic connections between photoreceptors and bipolar cells. The inner nuclear layer (INL) is composed of nuclei of bipolar, horizontal, and amacrine cells, exhibiting moderate cellular density. The inner plexiform layer (IPL) shows a fibrous appearance with synaptic networks, moderately stained due to neural processes. The ganglion cell layer (GCL) contains large neuronal cell bodies with clearly visible nuclei. The nerve fiber layer (NFL) consists of axons of ganglion cells, showing a compact arrangement. The internal limiting membrane (ILM) is seen as a thin boundary separating the retina from the vitreous body. Overall, Azan staining reveals preserved retinal architecture with distinct visualization of connective tissue elements and neural layers, suitable for quantitative morphometric assessment. Data are presented as mean ± standard deviation (SD). Morphometric evaluation of the retinal layers was performed using digital image analysis software (e.g., ImageJ, NIH, USA). Measurements included: Thickness of individual retinal layers (RPE, ONL, INL, IPL, GCL) total retinal thickness. Cell density in the ganglion cell layer (cells/mm<sup>2</sup>). For each animal, measurements were obtained from at least five non-overlapping microscopic fields per section at identical magnification. Mean values were calculated for each experimental group. Normality of data distribution was assessed using the Shapiro–Wilk test. For comparisons between multiple groups, one-way analysis of variance (ANOVA) followed by Tukey’s post hoc test was applied. In cases of non-normal distribution, the Kruskal–Wallis test followed by Dunn’s multiple comparisons test was used. A value of  $p < 0.05$  was considered statistically significant.

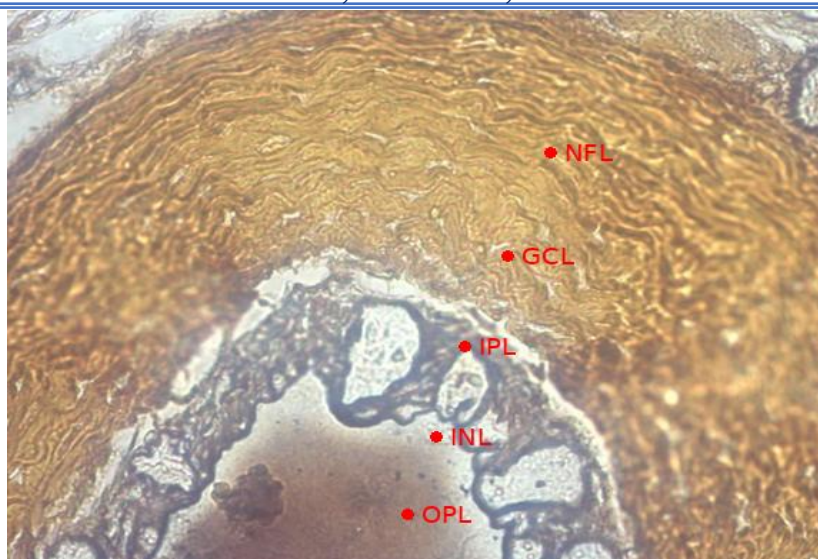


**Fig.2 Retina stained by Bielschowsky silver impregnation.**

1. NFL – Nerve fiber layer
2. GCL – Ganglion cell layer
3. IPL – Inner plexiform layer
4. INL – Inner nuclear layer
5. OPL – Outer plexiform layer
6. ONL – Outer nuclear layer
7. Photoreceptor layer

Fig.2 histological section of the retina stained using the Bielschowsky silver impregnation method demonstrates selective visualization of neuronal fibers and neurofibrillar structures, which appear dark brown to black against a lighter background. The nerve fiber layer (NFL) is prominently stained, revealing densely packed bundles of axons with a wavy, organized arrangement. The ganglion cell layer (GCL) is identified by large neuronal cell bodies with intensely impregnated neurofibrils. The inner plexiform layer (IPL) shows a dense network of argyrophilic neuronal processes forming synaptic connections. The inner nuclear layer (INL) contains moderately stained nuclei of bipolar, amacrine, and horizontal cells. The outer plexiform layer (OPL) appears as a thinner argyrophilic zone representing synaptic contacts between photoreceptors and bipolar cells. The outer nuclear layer (ONL) consists of rows of photoreceptor nuclei with weak silver impregnation. The photoreceptor layer is characterized by elongated, intensely impregnated axonal and dendritic processes, reflecting the integrity of retinal neuronal elements. Overall, Bielschowsky staining allows detailed assessment of the retinal neuronal architecture and neurofibrillar integrity, making it suitable for evaluation of neurodegenerative and experimental pathological changes.

**Results.** Disruption of normal retinal layer stratification was observed in the toxic hepatitis group compared with controls. Morphometric analysis revealed significant thinning of the outer nuclear layer (ONL) by 18%, a reduction in ganglion cell density by 22%, and thickening of the vascular wall by 35% ( $p < 0.05-0.01$ ). Periodic acid–Schiff (PAS) staining demonstrated pronounced glycoprotein accumulation within retinal vascular walls, indicating structural alterations of the basement membrane. In the silymarin-treated group, partial preservation of retinal architecture was observed, including reduced ONL thinning and lower vascular wall thickness compared with untreated animals, although parameters did not fully return to control values.

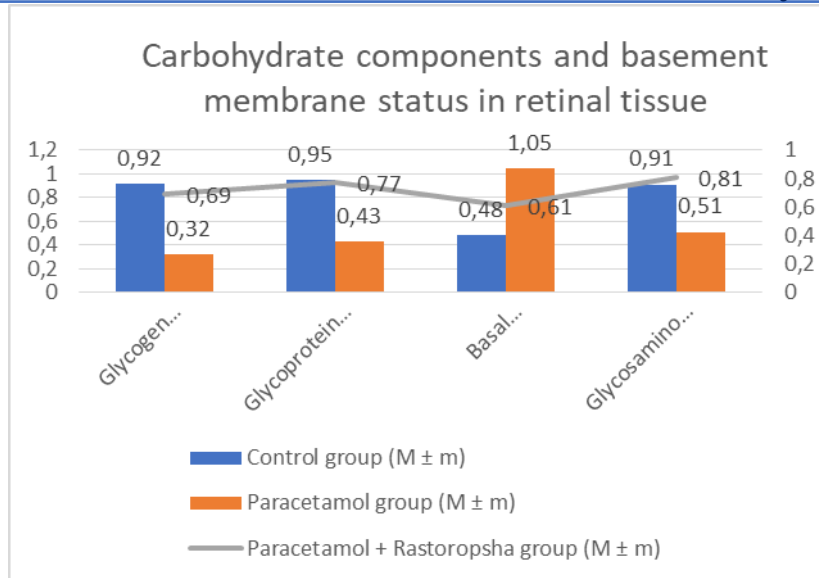


Table-1 Retinal sections were stained using: Hematoxylin and eosin (H&E) for general morphology, periodic acid–Schiff (PAS) reaction for glycoprotein detection, nissl staining for neuronal cell bodies, silver impregnation (Bielschowsky method) for neuronal fibers. Morphometric measurements were performed using digital image analysis software (ImageJ, NIH, USA). The following parameters were evaluated: thickness of retinal layers, ganglion cell density (cells/mm), vascular wall thickness (µm), measurements were obtained from at least five non-overlapping fields per section at identical magnification.

Statistical analysis was performed using GraphPad Prism software. Data are presented as mean ± standard deviation (SD). Normality was assessed using the Shapiro–Wilk test. Comparisons among groups were performed using one-way analysis of variance (ANOVA) followed by Tukey’s post hoc test. Differences were considered statistically significant at p < 0.05. Figure 1 The histological section of the retina stained with Azan trichrome demonstrates a clear stratified organization of retinal layers. Collagenous and connective tissue components are selectively stained blue, whereas cellular and cytoplasmic elements appear red to pink, allowing precise differentiation of retinal structures. The retinal pigment epithelium (RPE) forms a continuous outer layer adjacent to the choroid, showing moderate thickness and preserved integrity. The photoreceptor layer, including rods and cones, is distinguishable by elongated cellular elements oriented perpendicular to the retinal surface. Data are expressed as mean ± standard deviation (SD). Quantitative analysis was performed using ImageJ (NIH, USA). The following parameters were assessed: Thickness of NFL, IPL, and ONL (µm), density of argyrophilic fibers in the NFL (percentage area, %), number of ganglion cells per mm of retinal length, measurements were obtained from at least five randomly selected, non-overlapping fields per section at identical magnification. Normality was tested using the Shapiro–Wilk test. Comparisons among multiple groups were performed using one-way ANOVA followed by Tukey’s post hoc test. For non-normally distributed data, the Kruskal–Wallis test with Dunn’s multiple comparisons test was applied. Differences were considered statistically significant at p < 0.05. Morphometric parameters included retinal thickness, nuclear layer thickness, ganglion cell density, and vascular wall thickness. Data were analyzed using one-way ANOVA with Tukey post hoc test (p<0.05).

**Discussion.** The observed retinal alterations indicate that toxic hepatitis induces microvascular remodeling and neuronal degeneration in the retina, reflecting systemic metabolic and toxic imbalance. Vascular wall thickening and increased PAS positivity suggest basement membrane modification and early vascular sclerosis, consistent with microangiopathic changes. Degenerative

changes in the ganglion cell layer and thinning of the ONL point to retinal neuronal vulnerability under conditions of systemic toxicity. Hepatoprotective therapy with silymarin attenuated these pathological changes, supporting its partial protective effect, although complete normalization of retinal structure was not achieved.

**Conclusion and recommendation** Experimental toxic hepatitis induces profound microvascular disruption and progressive neurodegenerative remodeling in the retina, indicating that hepatic toxic injury extends beyond the liver to involve remote neurovascular tissues. Quantitative morphometric analysis demonstrated significant capillary rarefaction, endothelial degeneration, neuronal loss, and disorganization of retinal layers, supporting the concept of a liver–retina pathological axis. The partial structural preservation observed under hepatoprotective therapy suggests that systemic metabolic stabilization can attenuate, but not fully prevent, secondary retinal injury once hepatic toxicity is established. Collectively, these findings identify the retina as a highly sensitive morphological biomarker of systemic toxic damage and a potential surrogate tissue for assessing the severity and progression of hepatic injury.

Retinal morphometry should be considered as a supplementary experimental endpoint in studies of systemic toxic and hepatic injury. Early hepatoprotective intervention is recommended to reduce secondary neurovascular damage in extrahepatic organs, including the retina. Future studies should integrate digital image analysis and AI-assisted morphometry to improve sensitivity and reproducibility of retinal structural assessment. Multiorgan correlation analysis (liver–retina–brain axis) is warranted to elucidate mechanisms of systemic toxic propagation. Translation of retinal biomarkers into non-invasive clinical imaging (e.g., OCT-based morphometry) may enable early detection of hepatic-associated neurovascular injury in patients.

#### References:

1. Weber, L. W. D., Boll, M. & Stampfl, A. Hepatotoxicity and mechanism of action of haloalkanes: carbon tetrachloride as a toxicological model. *Crit. Rev. Toxicol.* **33**, 105–136 (2003).
2. Recknagel, R. O., Glende, E. A., Dolak, J. A. & Waller, R. L. Mechanisms of carbon tetrachloride toxicity. *Pharmacol. Ther.* **43**, 139–154 (1989).
3. Jaeschke, H., McGill, M. R. & Ramachandran, A. Oxidant stress, mitochondria, and cell death mechanisms in drug-induced liver injury. *Drug Metab. Rev.* **44**, 88–106 (2012).
4. Polyak, S. J., Morishima, C., Lohmann, V., Pal, S. & Lee, D. Y. Identification of hepatoprotective flavonolignans from silymarin. *Proc. Natl. Acad. Sci. U.S.A.* **107**, 5995–5999 (2010).
5. Vargas-Mendoza, N. et al. Hepatoprotective effect of silymarin. *World J. Hepatol.* **6**, 144–149 (2014).
6. Cunha-Vaz, J. The blood–retinal barriers system. Basic concepts and clinical evaluation. *Exp. Eye Res.* **78**, 715–721 (2004).
7. Antonetti, D. A., Klein, R. & Gardner, T. W. Diabetic retinopathy. *N. Engl. J. Med.* **366**, 1227–1239 (2012).
8. Osborne, N. N. et al. Retinal ischemia: mechanisms of damage and potential therapeutic strategies. *Prog. Retin. Eye Res.* **23**, 91–147 (2004).
9. Kolb, H., Fernandez, E. & Nelson, R. *Webvision: The Organization of the Retina and Visual System*. (University of Utah Health Sciences Center, 2019).